EUROPEAN ORGANIZATION FOR NUCLEAR RESEARCH
European Laboratory for Particle Physics

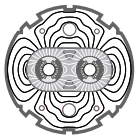

Large Hadron Collider Project **LHC Project Report 1051**

Layout design for final focus systems and applications for the LHC interaction region upgrade

Riccardo de Maria

Abstract

The design of a final focus system should aim in finding the best compromise between beam size and the maximum quadrupole gradient allowed by a given magnet technology. This article shows a method and a parametric layout that can be used as a design tool and allows relating the final focus limitations with the limits coming from magnet technologies. An application for the case of the LHC IR upgrade is shown.

Administrative Secretariat
LHC Division
CERN
CH-1211 Geneva 23
Switzerland

Geneva, September 2007

1 Introduction

Since the appearance of the alternating focusing theory ([1]) there have been attempts to find systematic tools to study the effect of multiplets of quadrupolar magnets on the beam phase space. One application is the design of a final focus system able to squeeze the transverse size of two particle beams in the interaction point (IP) of a circular collider and thereby to increase the interaction rate.

Several papers and reports have been written on this topic, (see [2], [3]), but the results, albeit useful as calculation tools for the analysis of a layout (in particular when the computational resources were limited), are not suited for the design process of a modern IR due to the complexity of the formulas which relate the layout parameters with the performance goals.

An approach, used in particular for linear collider by taking advantage of the symmetries in the layout and using thin lens approximation, (e.g. [4], [5] and more recently [6]) allows to optimize the chromatic and geometric aberrations by using non-linear elements and to achieve very small spot size, but leads to longer and more complex structures compared to the ones involving only linear elements. In circular colliders, this approach has not been yet proved to be satisfactory due to space limitations which does not allow efficient layouts and to a non-exact cancellation of the aberrations which limits the dynamic aperture (see [7]).

In recent years the SSC ([8]), the LHC ([9]) and its upgrade ([10]) triggered several studies for developing optimization tools for final focus systems. The high energy of the particles poses immediately a limit to the focusing capabilities of the superconducting magnets due the limited peak field that superconducting cables can sustain. Those studies were therefore motivated by the importance of understanding the performance limits (namely smallest possible beam size at the IP, aberrations, aperture margins) induced by a given magnet technology, not only for estimating the potential limitations of colliders but also as a feedback for the research in the magnet technology (see [11], [12], [13]).

These studies used several approximations (e.g. thin lens approximation in [14] and [15]) and restricted the analysis to some particular cases (e.g. coarse parameter scan for the SSC in [16] or symmetric triplets for the LHC in [14], [15] and [17]) in order to decrease the complexity of equation and reduce the dimensionality of the parameter space. On the other hand, this strategy exposes the studies to the chance of missing the true optimum and does not answer the question of what are the limitations induced by a magnet technology compared to the limitations of a given layout. In fact, the thin lens approximation is not always accurate and usually requires a refinement using the exact thick lens theory that spoils the generality of the results. A symmetric triplet is a layout that offers good performance close (e.g. in the nominal LHC), but not in all possible scenarios.

This article tries to overcome those limitations by introducing a parametric layout involving only quadrupoles whose performance (beam size at the IP, required peak field, chromatic aberrations) can be explored systematically for any possible situation.

The equations used here well approximate the exact thick lens theory. In case of round beams at the IP, they allow to relate the layout parameters to the performance goals through a set of univariate functions found numerically.

Report [17] shows a similar set of curves for a symmetric triplet layout, which are valid in a limited region of parameters.

The layout provides performance close to the best possible for a given magnet technology for round beams. Although the layout is not practical as is, small variation of

parameters allows designing a realistic layout with slightly lower performance.

The performance of the layout, being close to the best possible for a given technology, allows to link directly the limitations of a magnet technology with the limitations of a final focus system for round beams.

The optimization of a flat beam option is not covered by this paper because it relies on implementation details (e.g. beam screen) and physical effects (e.g. beam-beam effects) that are difficult to model in a general and scalable way. Nevertheless the strategy and the approximations presented here, being more general, could be used in such cases as well.

Section II presents the derivation of an approximated equation for the beam size used throughout the article. Section III shows an application of this equation for a constant gradient final focus system deriving some general properties. Those properties will be used in Sec. IV for writing a complete system of equations which relates the layout parameters with the basic performance of a particular type of focusing system. In addition Sec. IV, V and VI show the complete solution of the system of equations for several families of the focus system and a performance comparison between those families. Sections VII to XI present an application of the general results shown before to the case of the LHC IR upgrade. The parameter space for this case is extensively explored in order to identify the limitations of possible final focus system induced by the limits of the magnet technology.

2 Equation for the beam size

The purpose of a final focus system is to reduce the size of the beam as much as possible at a given position, i.e. interaction point (IP) in a collider, while leaving free space for the detector. The distance from the IP to the first quadrupole is called L^*.

In the paraxial approximation, the transverse coordinates of a particle in a pure quadrupole field follow the Hill's equation:

$$x''(s) + k(s)x(s) = 0, \tag{1}$$

where k is the normalized gradient and the derivative refers to the magnet longitudinal position s.

It is possible to determine the beam size of a monochromatic beam using the ansatz (see [1]):

$$x(s) = \sqrt{2I\beta(s)}\cos(\mu(s) + \phi) \tag{2}$$

where I and ϕ are the action and the initial phase of the particle and $\beta(s)$ and $\mu(s)$ are functions which follow the equations:

$$\frac{1}{2}\beta''(s)\beta(s) - \frac{1}{4}\beta'(s)^2 + k(s)\beta(s)^2 = 1 \tag{3}$$

$$\mu(s) = \int_{s_0}^{s} \frac{1}{\beta(s')}\mathrm{d}s'. \tag{4}$$

The RMS beam size σ of a beam can be expressed as:

$$\sigma = \sqrt{\varepsilon\beta} \tag{5}$$

where $\varepsilon =< I >$ is the emittance of the beam equal to the average action of the particles and β is the amplitude function, called the β-function.

For $k(s) = 0$ the Eq. (3) has the solution:

$$\beta(s) = \beta(s_0) - 2\alpha(s_0)(s - s_0) + \gamma(s_0)(s - s0)^2 \tag{6}$$

where $\beta(s_0)$, $\alpha(s_0) = -\beta'(s_0)/2$ and $\gamma(s_0) = (1 + \alpha(s_0)^2)/\beta(s_0)$ are the initial Twiss parameters.

Starting from the IP where $\beta(0) = \beta^*$ and β is minimal ($\beta'(0) = 0$), the beta function and the phase advance after the magnet free region at the beginning of the first quadrupole are given by:

$$\beta(L^*) = \beta^* + \frac{L^{*2}}{\beta^*} \tag{7}$$

$$\mu(L^*) = \arctan(\frac{L^*}{\beta^*}) \tag{8}$$

$$\simeq \frac{\pi}{2} - \frac{\beta^*}{L^*} + \frac{1}{3}\left(\frac{\beta^*}{L^*}\right)^3 + O\left(\left(\frac{\beta^*}{L^*}\right)^5\right). \tag{9}$$

If L^* is much bigger than β^*, the phase advance in this region is approximately $\frac{\pi}{2}$. This allows to approximate the function

$$\nu(s) = \sqrt{\beta(s)} \tag{10}$$

for $s >> \beta^*$ by the trajectory of a particle with initial phase equal to $\frac{\pi}{2}$ and initial conditions:

$$x(0) = 0 \qquad\qquad x'(0) = 1/\sqrt{\beta^*}. \tag{11}$$

The approximation continues to hold in the final focus system provided that $\beta(s)$ remains large with respect to the s coordinate, so that the contributions to the integral in Eq. (4) remain negligible.

In this approximation the equation for $\nu(s)$ is the same as for $x(s)$ that is:

$$\nu''(s) + k(s)\nu(s) = 0. \tag{12}$$

The same result can be found noting that the exact differential equation for $\nu(s)$ is

$$\nu''(s) + k(s)\nu(s) - \frac{1}{\nu^3(s)} = 0, \tag{13}$$

which follows from the ansatz

$$x(s) = \nu(s)e^{i\mu(s)} \tag{14}$$

and the following derivation (see [1]):

$$\nu'' + 2i\mu'\nu' + \nu(i\mu'' - \mu'^2 + k) = 0 \tag{15}$$

$$\nu'' - \nu\mu'^2 + \nu K = 0 \qquad 2\mu'\nu' + \nu\mu'' = 0 \tag{16}$$

$$\frac{\mu''}{\mu'} = -2\frac{\nu'}{\nu} \qquad D[\log(\mu')] = D[\log(\nu^{-2})] \tag{17}$$

$$\mu' = \frac{1}{\nu^2} \qquad \nu'' - \frac{1}{\nu^3} + \nu k = 0. \tag{18}$$

In the last equation, the term $1/\nu^3$ becomes negligible if k is bigger than $1/\nu^2$ or ν^2 is larger than the length of the focus system.

A solution of Eq. (12) for a positive and constant $k(s)$ is

$$\nu(s) = \nu_0 \cos(s\sqrt{k}) + \frac{\nu_0'}{\sqrt{k}} \sin(s\sqrt{k}) \tag{19}$$

and for a negative and constant $k(s)$ is

$$\nu(s) = \nu_0 \cosh(s\sqrt{k}) + \frac{\nu_0'}{\sqrt{k}} \sinh(s\sqrt{k}) \tag{20}$$

where ν_0 and ν_0' are the initial conditions.

A first application of this approximation can be the calculation of the maximum β inside a focusing quadrupole. If the approximation is valid, the maximum β in a quadrupole, if this maximum is not trivially on one of the two extremities, can be found solving the system:

$$\nu_m = \nu(s_m) = \nu_0 \cos(s_m\sqrt{k}) + \frac{\nu_0'}{\sqrt{k}} \sin(s_m\sqrt{k}) \tag{21}$$

$$0 = \nu'(s_m) = -\nu_0\sqrt{k} \sin(s_m\sqrt{k}) + \nu_0' \cos(s_m\sqrt{k}). \tag{22}$$

which is equivalent to

$$\tan(s_m\sqrt{k}) = \frac{\nu_0'}{\nu_0\sqrt{k}} = -\frac{\alpha_0}{\beta_0\sqrt{k}} \tag{23}$$

$$\beta_m = \nu_m^2 = \nu_0^2 + \left(\frac{\nu_0'}{\sqrt{k}}\right)^2 = \beta_0 + \frac{\alpha_0^2}{\beta_0 k} \tag{24}$$

where $\beta_m = \nu_m^2$ is the maximum β, s_m is the location where the maximum occurs, $\nu_0 = \sqrt{\beta_0}$ and $\nu_0' = -\alpha_0/\nu_0$ are the initial conditions at the beginning of the quadrupole.

3 Constant gradient final focus

It is possible to construct a simple parametric layout for a final focus which can be completely solved and is already close to an optimal final focus in terms of minimum beam size for a given peak field.

The layout consists of a piecewise constant gradient which assumes only two values:

$$k(s) = ak \tag{25}$$

where k is a positive number and $a = \pm 1$ for a focusing quadrupole and for a defocusing one, respectively.

It is possible to introduce a function $w(\theta)$ using the transformations:

$$\theta \to s\sqrt{k} \tag{26}$$

$$\nu(s) \to \nu(\theta/\sqrt{k}) \equiv w(\theta) \tag{27}$$

$$\nu'(s) \to \sqrt{k} w'(\theta) \tag{28}$$

$$\nu''(s) \to k w''(\theta). \tag{29}$$

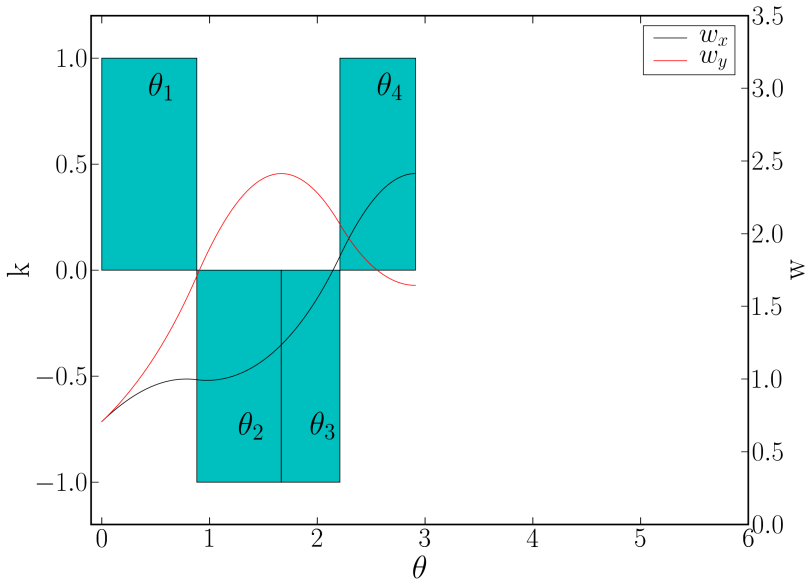

Figure 1: Point to parallel constant gradient triplet with initial condition $w_0 = \sin(\theta_0), w_0' = \cos(\theta_0), \theta_0 = \pi/4$. The boxes represent the position, length and polarity of the quadrupoles. The curves show $w = \sqrt{\beta}$ as function of the normalized longitudinal position $\theta = s\sqrt{k}$. A scaling of the initial condition translates into scaling w while keeping the same lengths for the quadrupoles (Property 1). The solution remains unchanged if $k \to \alpha k$, $\theta \to \theta/\alpha$, $w_0' \to \alpha w_0'$.

The function $w(\theta)$ follows the differential equation

$$w''(\theta) + aw(\theta) = 0. \tag{30}$$

The solution can be written, respectively for $a = 1$ and $a = -1$, as:

$$\begin{pmatrix} w(\theta) \\ w'(\theta) \end{pmatrix} = R(\theta) \begin{pmatrix} w_0 \\ w_0' \end{pmatrix} \tag{31}$$

$$\begin{pmatrix} w(\theta) \\ w'(\theta) \end{pmatrix} = H(\theta) \begin{pmatrix} w_0 \\ w_0' \end{pmatrix} \tag{32}$$

where $R(\theta)$ and $H(\theta)$ are circular and hyperbolic rotations:

$$R(\theta) = e^{\theta J} = \begin{pmatrix} \cos(\theta) & \sin(\theta) \\ -\sin(\theta) & \cos(\theta) \end{pmatrix} \qquad J = \begin{pmatrix} 0 & -1 \\ 1 & 0 \end{pmatrix} \tag{33}$$

$$H(\theta) = e^{\theta S} = \begin{pmatrix} \cosh(\theta) & \sinh(\theta) \\ \sinh(\theta) & \cosh(\theta) \end{pmatrix} \qquad S = \begin{pmatrix} 0 & 1 \\ 1 & 0 \end{pmatrix} \tag{34}$$

The following presents some general properties arising from the approximated Eq. (12) which can be used for writing a complete system of equations for design of a layout.

3.1 Property 1

As $w(\theta)$ follows a linear homogeneous equation, the solution for a given initial condition is still a solution of the differential equation after a rescaling of the type:

$$w \to \alpha w. \tag{35}$$

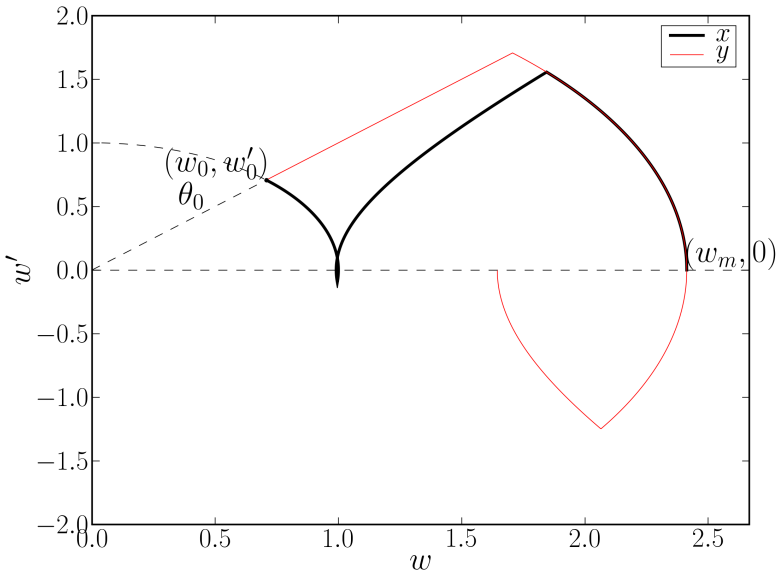

Figure 2: Phase space diagram for a point to parallel constant gradient triplet with initial condition $w_0 = \sin(\theta_0), w_0' = \cos(\theta_0), \theta_0 = \pi/4$. The curves show $w = \sqrt{\beta}$ in the (w, w') space. The black curve (x) is composed by a sequence of a circular, hyperbolic and again circular rotation which represents a sequence of a focusing, defocusing and again focusing quadrupole. The red curve on the contrary (y) is composed by a hyperbolic, circular and hyperbolic rotations. The circular rotation for the y coordinate and the last circular rotation for x on the right side of the figure overlaps because one has imposed that $\max(\beta_x) = \max(\beta_y)$. The point $(w_m, 0)$ identifies the maximum β.

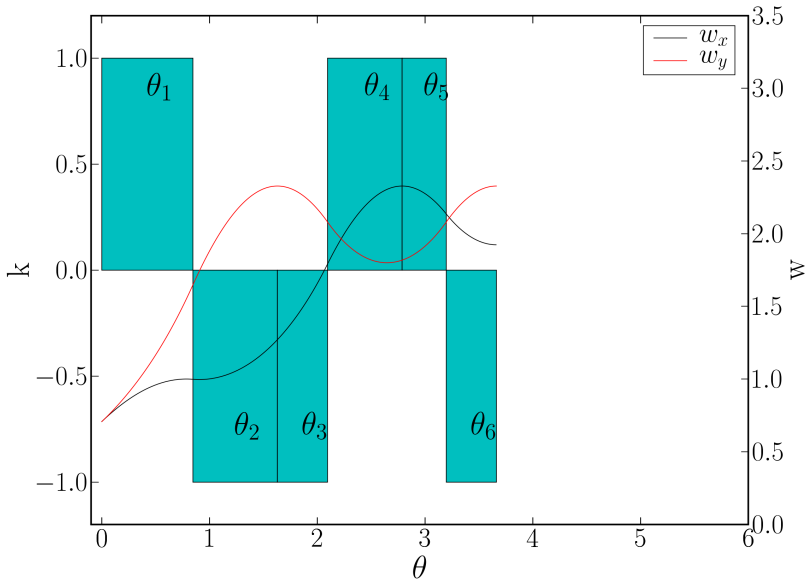

Figure 3: Point to parallel constant gradient quadruplet with initial condition $w_0 = \sin(\theta_0), w_0' = \cos(\theta_0), \theta_0 = \pi/4$. The boxes represent the position, length and polarity of the quadrupoles. The curves show $w = \sqrt{\beta}$ for a normalized gradient as function of the normalized longitudinal position $\theta = s\sqrt{k}$. A scaling of the initial condition translates into scaling w while keeping the same lengths for the quadrupoles (Property 1). The solution is unchanged if $k \to \alpha k$, $\theta \to \theta/\alpha$, $w_0' \to \alpha w_0'$.

Therefore all the possible solutions of a given problem depend only on one parameter θ_0 and can be represented as:

$$w(0) = \sin(\theta_0) \tag{36}$$
$$w'(0) = \cos(\theta_0). \tag{37}$$

This property can be used to scale the solutions for identical systems whose initial conditions are linearly dependent.

3.2 Property 2

For a defocusing and focusing doublet with the initial conditions:

$$w(0) = \sin(\theta_0) \tag{38}$$
$$w'(0) = \cos(\theta_0) \tag{39}$$

and normalized lengths $\theta_1 = l_1\sqrt{k}$, $\theta_2 = l_2\sqrt{k}$, the maximum β in the doublet is:

$$\beta_m = w_m^2 = \left| H(\theta_1) \begin{pmatrix} \sin(\theta_0) \\ \cos(\theta_0) \end{pmatrix} \right| = \tag{40}$$
$$= \cosh(2\theta_1) + \sin(2\theta_0)\sinh(2\theta_1) \tag{41}$$

where $||$ is the Euclidean distance.

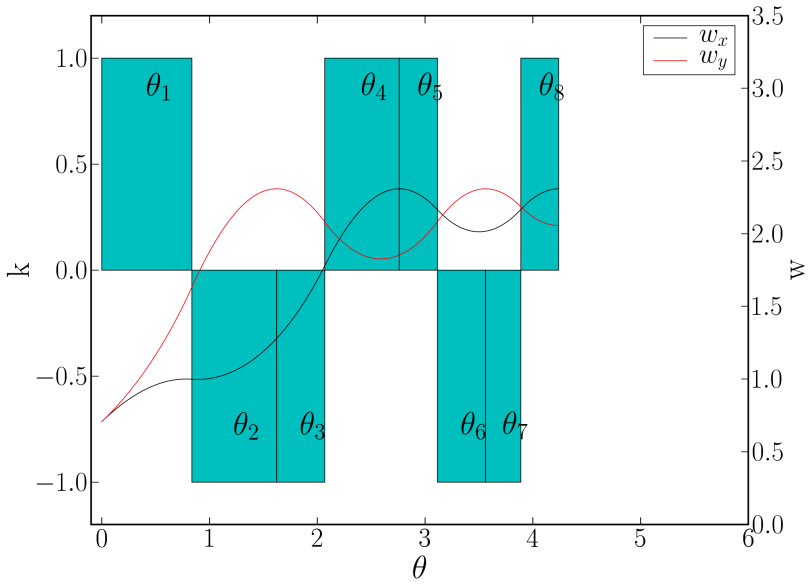

Figure 4: Point to parallel constant gradient quintuplet with initial condition $w_0 = \sin(\theta_0), w_0' = \cos(\theta_0), \theta_0 = \pi/4$. The boxes represent the position, length and polarity of the quadrupoles. The curves show $w = \sqrt{\beta}$ as function of the normalized longitudinal position $\theta = s\sqrt{k}$. A scaling of the initial condition translates into scaling w while keeping the same lengths for the quadrupoles (Property 1). The solution is unchanged if $k \to \alpha k$, $\theta \to \theta/\alpha$, $w_0' \to \alpha w_0'$.

The last equation can be rewritten as

$$\tanh(\theta_1) = \frac{-\sin(\theta_0) + \sqrt{\beta_m^2 + \cos^2(\theta_0)}}{1 + \beta_m}. \tag{42}$$

This property can be applied to the configurations shown in Fig. 1 and Fig. 2. Figure 1 shows an arrangement of two doublets. The boxes represent the position, length and gradient of the quadrupole and the curves represent the w-function. The first two elements are a defocusing and focusing doublet in the y-plane. The maximum of the w-function (red line) can be calculated using the quantities θ_0 and θ_1 and Eq. 41. Figure 2 shows the same system in a phase space diagram. The hyperbolic and circular rotations start from the point $(w_0 = \sin\theta_0, w_0' = \cos\theta_0)$. The point $(w_m, w_0' = 0)$ identifies the maximum of the w-function.

3.3 Property 3

Under the same conditions of the last property and for $w' = 0$ at the end of the doublet, we have:

$$\theta_2 = \arg\left(H(\theta_1)\begin{pmatrix}\sin(\theta_0)\\ \cos(\theta_0)\end{pmatrix}\right) \tag{43}$$

which is equivalent to

$$\tan(\theta_2) = \frac{1 + \tan(\theta_0)\tanh(\theta_1)}{\tan(\theta_0) + \tanh(\theta_1)}. \tag{44}$$

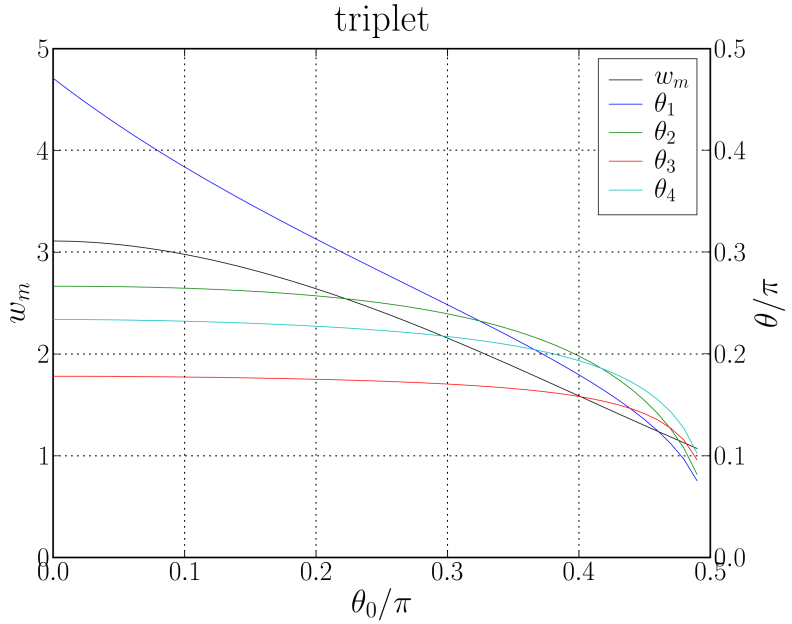

Figure 5: Solution for a triplet final focus system. The figure shows the normalized lengths $\theta_i = l_i\sqrt{k}$ and the maximum $w = \sqrt{\beta}$ as a function of the initial conditions parameterized according to $w_0 = \sin(\theta_0), w_0' = \cos(\theta_0)$.

For instance θ_2 in Fig. 1 can be calculated using Eq. (44) because $w_y' = 0$ at the end of the second quadrupole.

3.4 Property 4

For a focusing and defocusing doublet with normalized lengths θ_3, θ_4 and $w' = 0$ at the beginning and the end,

$$\tan(\theta_3) = \tanh(\theta_4). \tag{45}$$

For instance θ_3 and θ_4 in Fig. 1 follow this property because $w_y' = 0$ at the beginning of the third quadrupole (focusing in the y-plane) and the end of the fourth quadrupole (defocusing in the y-plane).

4 Constant gradient point to parallel focusing

The previous properties are sufficient to find the equations for a constant gradient point to parallel triplet with normalized lengths $\theta_1, \theta_2 + \theta_3, \theta_4$, initial condition θ_0 and $\beta_m = \max(\beta_x) = \max(\beta_y)$.

The equations are:

$$\tan(\theta_2) = \frac{1 + \tan(\theta_0)\tanh(\theta_1)}{\tan(\theta_0) + \tanh(\theta_1)} \tag{46}$$

$$\beta_m = \cosh(2\theta_1) + \sin(2\theta_0)\sinh(2\theta_1) \tag{47}$$

$$\tan(\theta_3) = \tanh(\theta_4) \tag{48}$$

$$\tanh(\theta_2 + \theta_3) = \frac{-\sin(\theta_0 + \theta_1) + \sqrt{\beta_m^2 + \cos^2(\theta_0 + \theta_1)}}{1 + \beta_m} \tag{49}$$

$$\tan(\theta_4) = \frac{1 + \tan(\theta_0 + \theta_1)\tanh(\theta_2 + \theta_3)}{\tan(\theta_0 + \theta_1) + \tanh(\theta_2 + \theta_3)}. \tag{50}$$

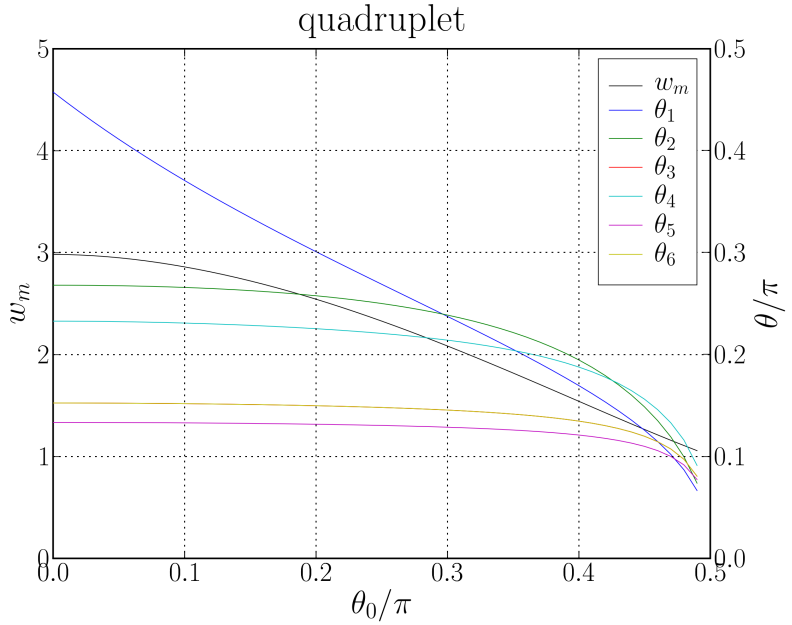

Figure 6: Solution for a quadruplet final focus system. The figure shows the normalized lengths $\theta_i = l_i\sqrt{k}$ and the maximum $w = \sqrt{\beta}$ as a function of the initial conditions parameterized according to $w_0 = \sin(\theta_0), w_0' = \cos(\theta_0)$.

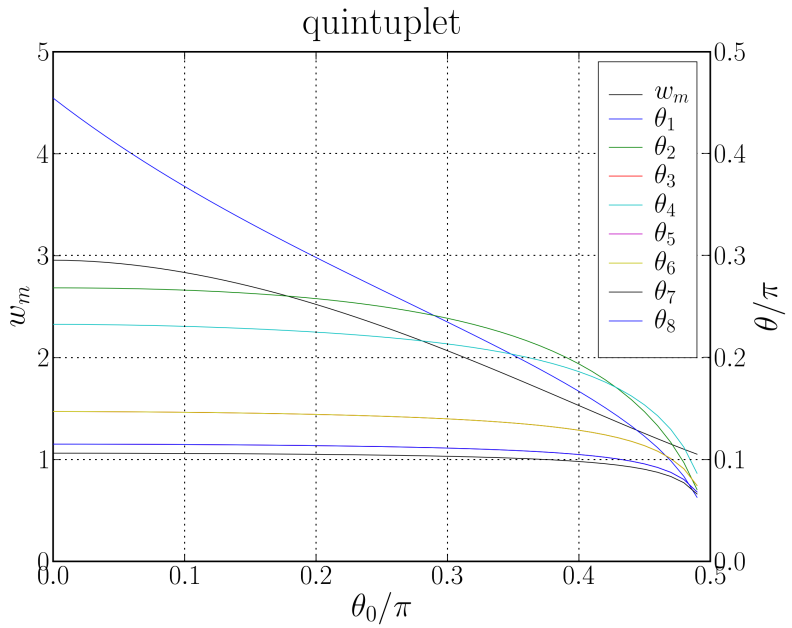

Figure 7: Solution for a quintuplet final focus system. The figure shows the normalized lengths $\theta_i = l_i\sqrt{k}$ and the maximum $w = \sqrt{\beta}$ as a function of the initial conditions parameterized according to $w_0 = \sin(\theta_0), w_0' = \cos(\theta_0)$.

A solution for $\theta_0 = \pi/4$ is shown in Fig. 1. A complete set of solutions of θ_i and β_m as a function of θ_0 can be found in Fig. 5. It is worth noting that the normalized lengths of the first element is much more sensible on the initial condition that the other lengths. There is only one particular initial condition which generates a symmetric triplet (i.e. $\theta_0 \simeq 0.7$ when $\theta_1 = \theta_4$). For θ_0 bigger than this value the layout remains approximately symmetric, while for θ_0 smaller the layout starts to loose the symmetry.

For a quadruplet a similar set of functions can be found by eliminating the last equation and adding:

$$\tan(\theta_6) = \tanh(t6) \tag{51}$$

$$\theta_3 = \theta_6 \tag{52}$$

$$\tan(\theta_3) = \tanh((\theta_5 + \theta_4)/2). \tag{53}$$

A solution for $\theta_0 = \pi/4$ is shown in Fig. 3. A complete solution as a function of θ_0 can be found in Fig. 6. The lengths of $\theta_1, \theta_2, \theta_4$ remain approximately the same with respect to the triplet solution, while θ_3 is reduced. This layout shows a slightly smaller peak of w (yielding a smaller beam size) compared to the triplet solution.

The system can be extended to any multiplet. A quintuplet is shown in Fig. 4 and Fig. 7. The quintuplet shows no improvement in terms of beam size compared to the previous solution, while increasing the number of magnetic elements. A larger number of elements follow this trend; the only effect is to progressively reduce the difference between w_x and w_y which is in most of the case an unwanted feature.

Those layout families have the property to be at the border between a focusing and defocusing system while minimizing the peak beta function and therefore the chromatic aberrations. The layout has no gaps between the quadrupole, numerical evidences (see also [16]) show that the presence of gaps results in a layouts featuring a larger peak beta function and chromatic aberrations with respect to a gap-less layout. This fact and the results presented indicate that the peak beta function of this layout is the global minimum for every possible focusing system.

The layout is not a practical final focus system as it is, but a small variation of the parameters and the addition of gaps between the quadrupoles allows it to become a realistic final focus system at the cost of an increase of the peak beta function.

5 Performance comparison

Figures 8, 9 and 10 show a comparison between the multiplets according to their maximum β. Figure 8 shows that, for the same initial conditions, the quadruplet features a smaller peak beta function than the triplet, while the gain is rather small passing from a quadruplet to a quintuplet and multiplets with a large number of elements. Figure 9 shows clearly that the total length increases with the number of elements.

A relevant figure of merit is the contribution to the chromatic aberration of a final focus system. It is proportional to the integral:

$$Q' = -\frac{1}{4\pi} \int \beta k ds. \tag{54}$$

The integral can be calculated using the solution for $\beta(s)$

$$\sqrt{\beta} = w_c(\theta) = w_0 \cos(\theta) + w_0' \sin(\theta) \qquad \text{for} \quad k = 1 \tag{55}$$

$$\sqrt{\beta} = w_h(\theta) = w_0 \cosh(\theta) + w_0' \sinh(\theta) \qquad \text{for} \quad k = -1. \tag{56}$$

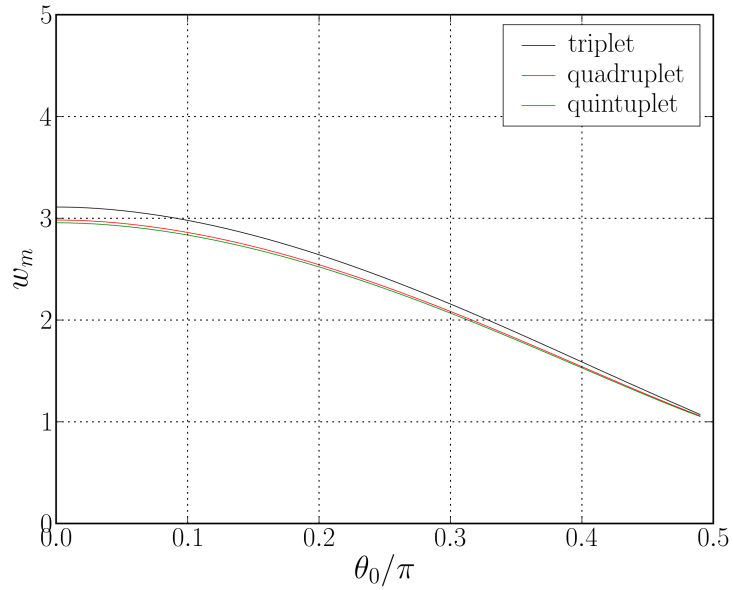

Figure 8: Comparison of the maximum $w = \beta$ inside the quadrupole for a point to parallel constant gradient focusing. The curves represent the solution for a triplet, quadruplet, quintuplet solution as a function of initial conditions parameterized according to $w = \sin(\theta_0), w' = \cos(\theta_0)$.

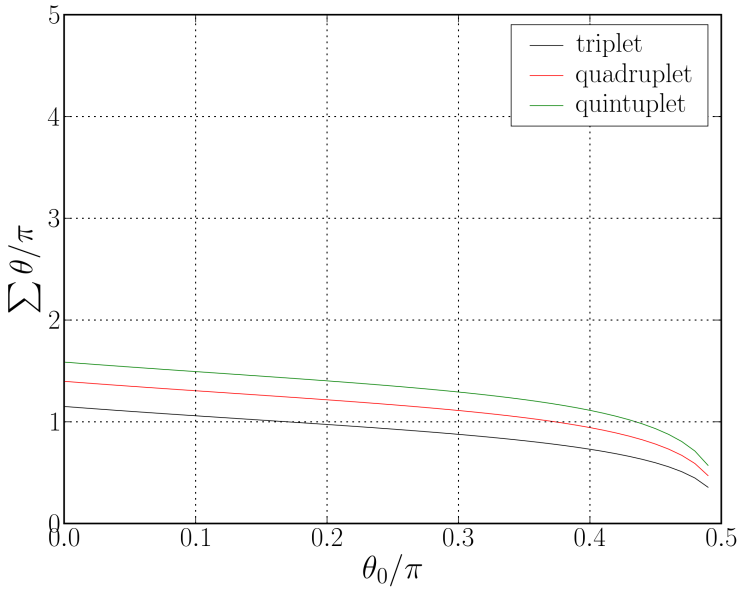

Figure 9: Comparison of the total length of a final focus system. The curves represent the solution for a triplet, quadruplet, quintuplet solution as a function of initial conditions parameterized according to $w = \sin(\theta_0), w' = \cos(\theta_0)$.

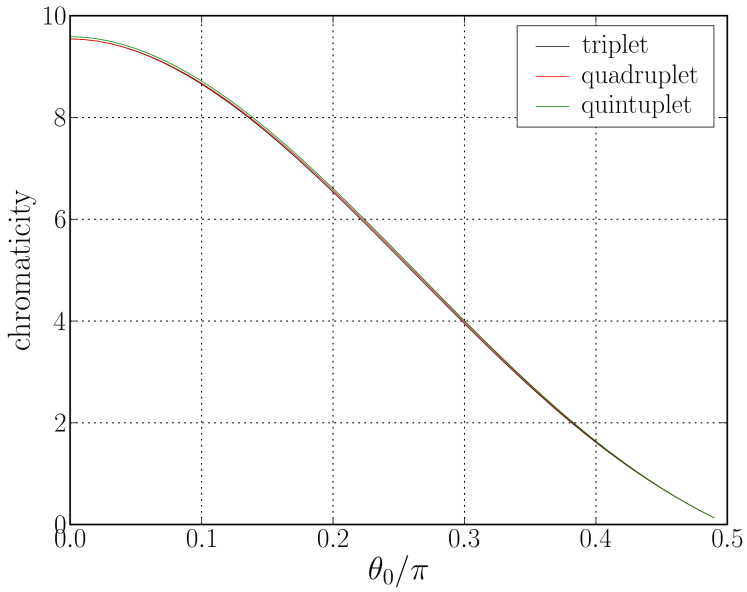

Figure 10: Comparison of the chromaticity of a final focus system. The curves represent the solution for a triplet, quadruplet, quintuplet solution as a function of initial conditions parameterized according to $w = \sin(\theta_0), w' = \cos(\theta_0)$.

Therefore the integral can be evaluated by summing up the following parts:

$$4\pi Q' = -\int_0^\theta w_c^2(\theta')\mathrm{d}\theta' = \tag{57}$$

$$= -\frac{(w_0^2 + {w_0'}^2)\theta + w_0 w_0'}{2} \tag{58}$$

$$+ \frac{w_0 w_0'}{2}\cos(2\theta) - \frac{w_0^2 - {w_0'}^2}{4}\sin(2\theta) \tag{59}$$

for $k = 1$ and

$$4\pi Q' = \int_0^\theta w_h^2(\theta')\mathrm{d}\theta' = \tag{60}$$

$$= \frac{(w_0^2 - {w_0'}^2)\theta - w_0 w_0'}{2} \tag{61}$$

$$+ \frac{w_0 w_0'}{2}\cosh(2\theta) + \frac{w_0^2 + {w_0'}^2}{4}\sin(2\theta) \tag{62}$$

for $k = -1$.

Figure 10 shows the average of the chromatic integral for both planes. The chromaticity is almost identical for any multiplet.

The comparisons show that increasing the number of magnetic elements in a final focus system does not increase the performance (peak beta function and chromatic aberration) while increasing the length and therefore the cost. Only triplet and to some extent a quadruplet (slightly lower peak beta function) represent suitable layouts for a compact final focus system for round beams.

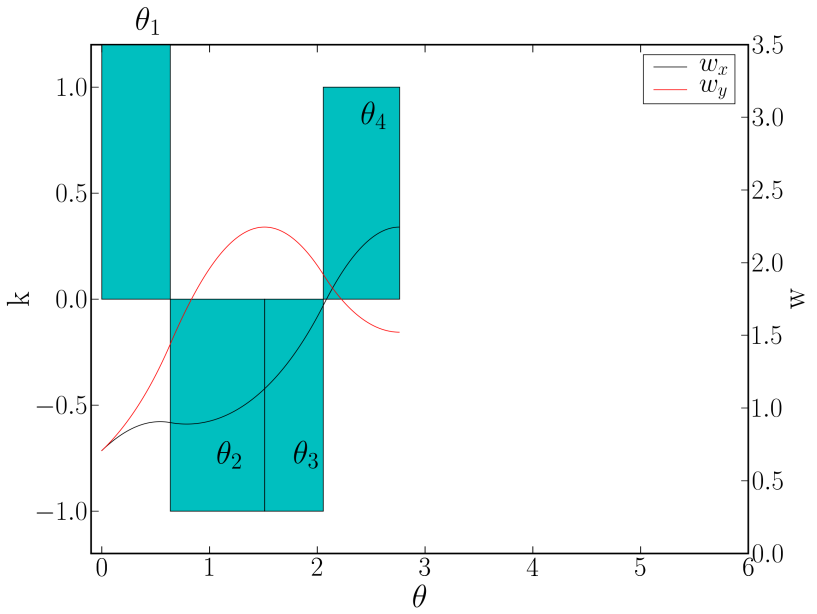

Figure 11: Optimized triplet solution, where the gradient of the first quadrupole is larger than the other but keeping the same product $w_m k$ (which is proportional to the minimum required pole field) where w_m indicates the maximum inside the quadrupoles.

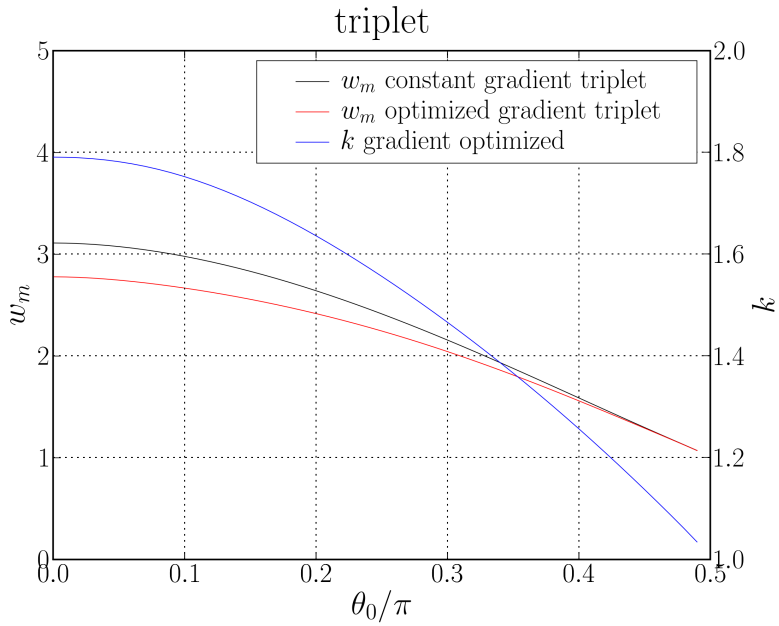

Figure 12: Comparison of the maximum $w = \beta$ inside the quadrupole for a point to parallel focusing system. The curves represent the solution for a constant gradient triplet and an optimized gradient triplet as function of initial conditions parameterized according to $w = \sin(\theta_0), w' = \cos(\theta_0)$. The blue line is the ratio between the gradient of the first quadrupole and the gradient of the other quadrupoles for the optimized gradient triplet. The solution is optimized such that the maximum field at 1σ in the first quadrupole is the same with respect to the one in the other quadrupoles. The gradient of the first quadrupole is larger because the beam size, which is proportional to w, is smaller.

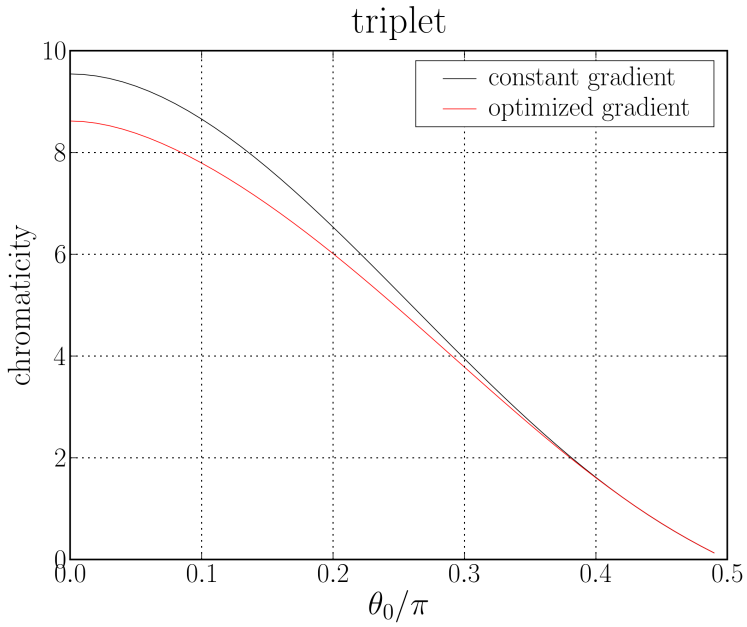

Figure 13: Comparison of the chromaticity of final focus systems. The curves represent the solution for a constant gradient triplet and an optimized gradient triplet as a function of initial conditions parameterized according to $w = \sin(\theta_0), w' = \cos(\theta_0)$. The optimized gradient triplet has a smaller chromaticity compared to a constant gradient triplet.

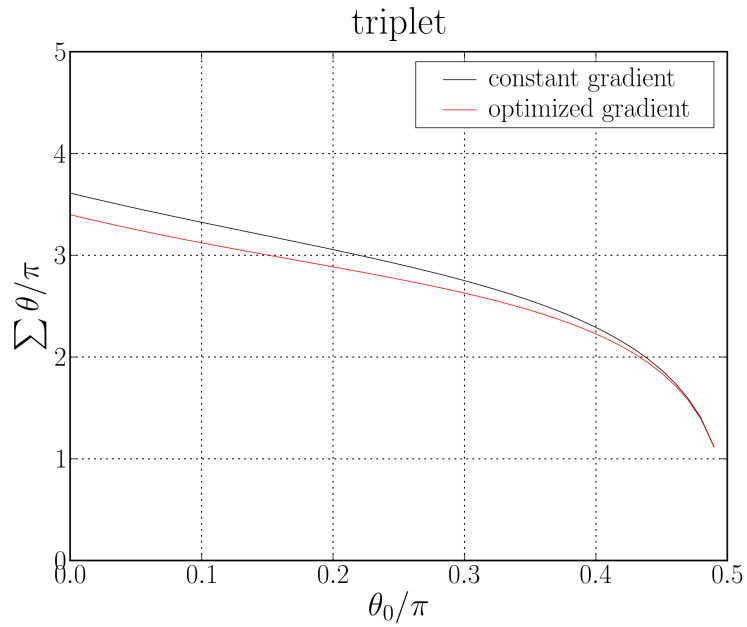

Figure 14: Comparison of the total length of final focus systems. The curves represent the solution for a constant gradient triplet and an optimized gradient triplet as a function of initial conditions parameterized according to $w = \sin(\theta_0), w' = \cos(\theta_0)$. The optimized gradient requires a smaller length compared to a constant gradient triplet.

6 Optimized gradient final focus

The previous results show that in all the constant gradient final focus systems, the first quadrupole has always the smallest beam size. At the cost of a specialized magnet with a smaller aperture and a larger gradient but with the same pole field ($\propto wk$), it is possible to push the performance a bit further. As an example Fig. 11 shows an optimized triplet that features a larger gradient for the first quadrupole allowing a reduction of the peak beta function, while keeping the same peak field in the coil (i.e. keeping the same magnet technology) by reducing the mechanical aperture.

Figure 12 shows the gain in maximum beta function and the corresponding increase of the gradient.

Figures 13 and 14 shows the gain in terms of chromaticity and total length.

The option of a specialized first magnet with a different technology has been proposed also in [18] which yields even better performance. The analysis of mixed technology, while being an interesting option, is out of the scope of this article.

7 Estimates for the LHC upgrade

As soon as the LHC reaches its nominal performance the present triplet magnets will be close to their performance limit. An upgrade of the interaction region (IR) together with a better understanding of the machine will be required for a further increase of the LHC performance (see [19], [11], [12], [13]).

Using the results from the previous chapter we can explore systematically the options for an upgrade using the existing NbTi technology and the new Nb_3Sn technology. In the following we will use the results of the previous chapter together with some empirical estimates to draw a region in the parameter space compatible with the technology and operation limits of the LHC.

8 Aperture limit

In case of the LHC, it is possible to give a crude estimate of the required transverse mechanical aperture using:

$$d_p = 33\sigma + 22 \text{ mm} \tag{63}$$

where d_p is the inner coil diameter, σ is the RMS beam size and 22 mm is an empirical quantity which takes the mechanical tolerances of the magnet and the closed orbit, the beam screen and the beam pipe into account (see [20]).

Knowing the gradient g of the magnet we can calculate the pole field:

$$B_p = \frac{1}{2} g d_p. \tag{64}$$

A rough estimate for B_p is $B_p < 6.5$ T for a NbTi magnet and $B_p < 12$ T for a Nb_3Sn one.

A refined scaling can be found in [21].

Figure 15 shows the region of (beta, gradient) values compatible with the different technologies.

9 Aberration limit

The aberrations reduce the size of the stable beam. They are proportional to some power of the beta function and may depend in a non trivial way on the field quality of the

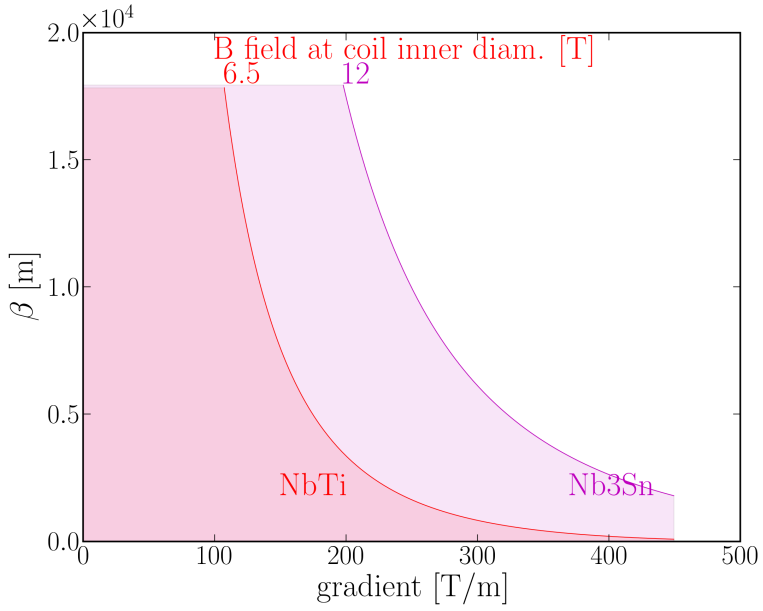

Figure 15: Pole field limit. The figure show the regions in the (maximum β, gradient) space, where it is possible to find a solution for a final focus system for which the magnets have a pole field of 6.5 T (compatible with the NbTi technology) and 12 T (compatible with Nb_3Sn technology).

magnet. It is difficult to find an empirical law which sets a limit for the beta function and field quality. Experience shows that with a beta function larger than 18 km in the final focus magnets one reaches the limits for the chromaticity correction and observes severe limitations on the dynamic aperture (see [7], [22]).

10 Focus limit

Previous experience shows that a constant gradient, gap-less, final focus is a good model for a realistic final focus for the LHC. It gives a good estimate of the minimum beta function that a final focus can achieve with a given quadrupole gradient and β^*.

Using a different parameterization than the one shown in the previous part, it is possible to find scaling laws for a final focus system which directly relate β^*, L^* with the specification of the final focus system.

For a given β^* and L^* at the IP the initial conditions in normalized coordinates are:

$$w_0 = w(\theta = 0) = L^*/\sqrt{\beta^*} \tag{65}$$

$$w_0' = w(\theta = 0) = w'(s = 0)/\sqrt{k} = 1/\sqrt{k\beta^*}. \tag{66}$$

If we use the dimensionless initial conditions:

$$w_0 = L^*\sqrt{k} \tag{67}$$

$$w_0' = 1 \tag{68}$$

and Property 1 for scaling the solutions, it is possible to find the lengths of the quadrupoles and the maximum beta for a final focus system from the normalized quantities $\theta_i(w_0)$ and

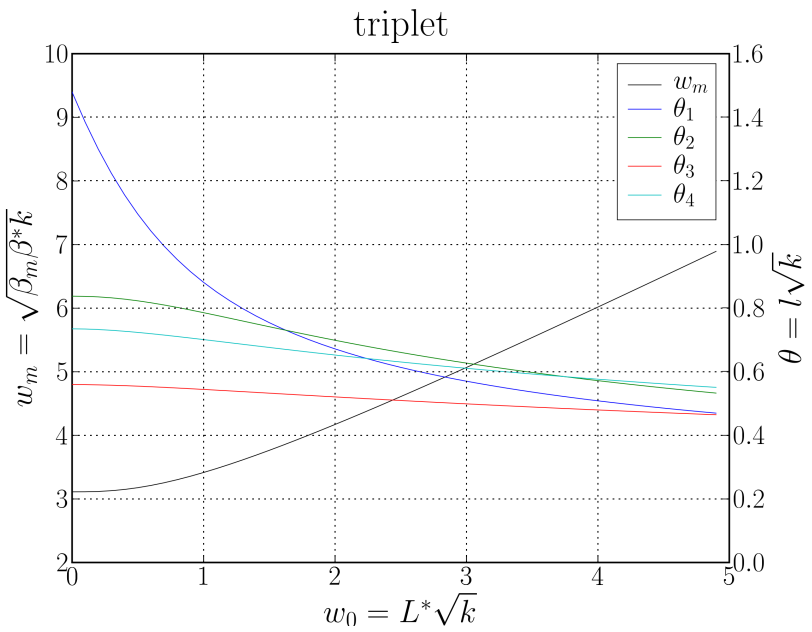

Figure 16: Solution for a triplet final focus system. Figure shows the normalized lengths $\theta_i = l_i\sqrt{k}$ and the maximum $w = \sqrt{\beta}$ as a function of the initial conditions parameterized according to $w = L^*\sqrt{k}, w' = 1$. The solution can be scaled to any β^*, L^*, k according to the equations shown in the labeling of the axis.

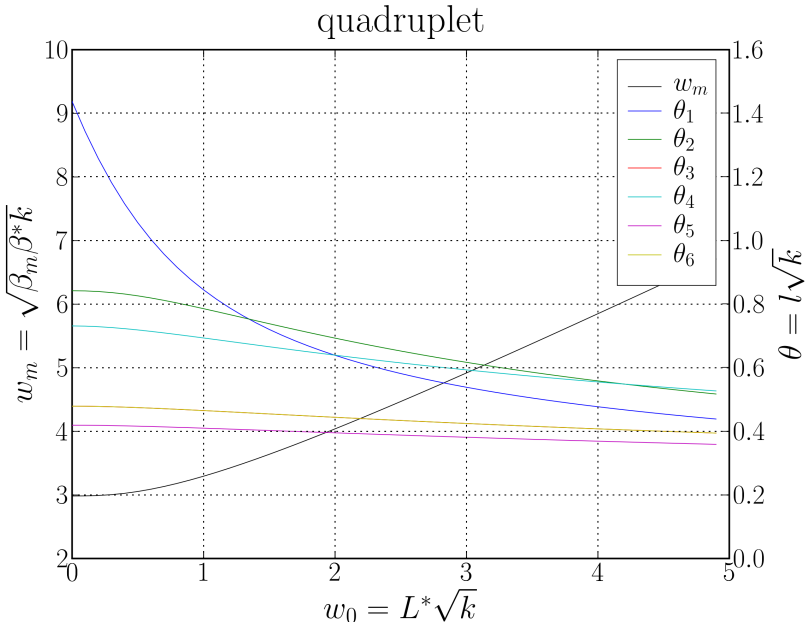

Figure 17: Solution for a quadruplet final focus system. Figure shows the normalized lengths $\theta_i = l_i\sqrt{k}$ and the maximum $w = \sqrt{\beta}$ as a function of the initial conditions parameterized according to $w = L^*\sqrt{k}, w' = 1$. The solution can be scaled to any β^*, L^*, k according to the equations shown in the labeling of the axis.

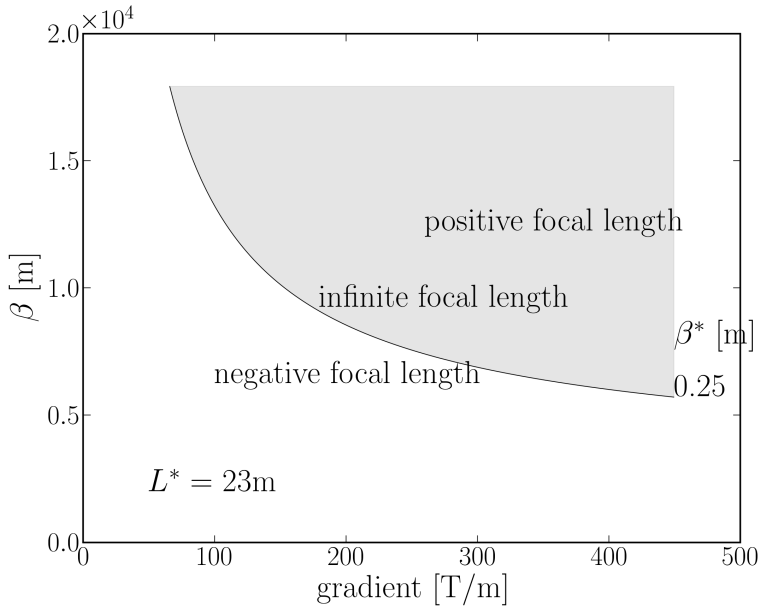

Figure 18: Focus limit. The figure shows the region in the (maximum β, gradient) space, where it is possible to find a solution for a triplet final focus system for the LHC given $L^* = 23$ m and $\beta = 25$ cm. The gray area indicates the parameters of a triplet that can focus in both planes. The curve shows the minimal β peak for a constant gradient focus system as a function of the gradient.

$w_m(w_0)$:

$$l_i = \theta_i/\sqrt{k} \tag{69}$$

$$\beta_m = \frac{w_m^2}{k\beta^*} \tag{70}$$

The functions $\theta_i(w_0)$ and $w_m(w_0)$ can be evaluated numerically as in the previous chapter. The solutions for a triplet and a quadruplet are shown in Fig. 16 and 17.

Those plots represent the scaling laws when the variables are transformed to the real parameters. The results are general and can be used for the design of any final focus system for which one wants optimize the compactness and the quadrupole peak field.

In case of the LHC, for which $w_0 = L^*\sqrt{k} \simeq 2.3$, Fig. 16 shows that a symmetric triplet represent an optimum ($\theta_1 = \theta_4$), while is not more the case for a smaller L^*.

Choosing a value for L^* and β^* (e.g. $L^* = 23$ m and 0.25 m for the case of the LHC upgrade), it is possible to show (see Fig. 18) the region of the parameters gradient and peak beta function for which a constant gradient triplet can focus a round beam in both planes. In other words from this plot it is possible to estimate which is the minimum gradient needed to design a final focusing system which features a given peak of the beta function. In fact, the necessary variations, for transforming the limit case in a realistic design (i.e. positive focal length, gaps between quadrupoles), have the effect of increasing the peak beta function. Such an increase can be partially recovered by optimizing the first quadrupole (see Sec. VI and Sec. XI) or move to a quadruplet solution at the cost of more magnets.

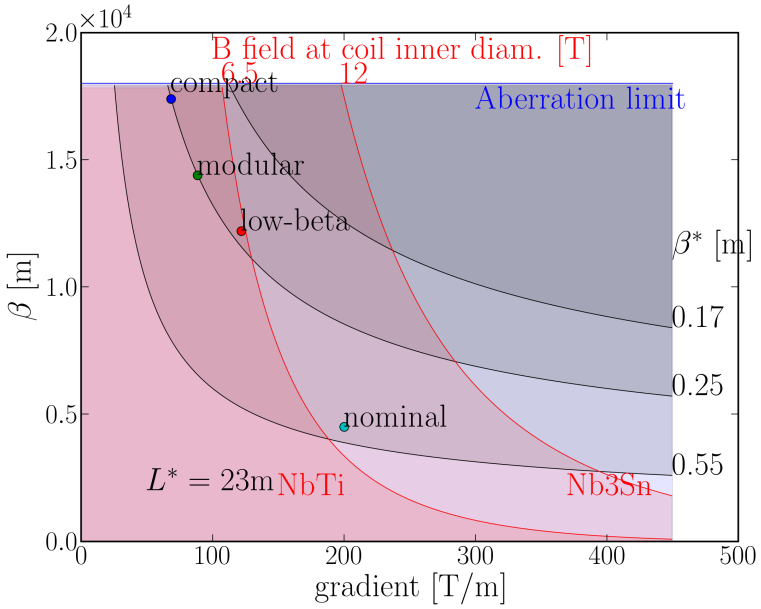

Figure 19: LHC upgrade. The figure shows the region in the maximum (β, gradient)-space, where it is possible to find a solution for a triplet final focus system for the LHC. The combination of red and gray shades show the parameter regions delimited by the pole field in the magnet (regions below the red lines) and the focusing ability (regions above the gray lines). The points represent some realistic upgrade layouts presented in [20] and the nominal LHC.

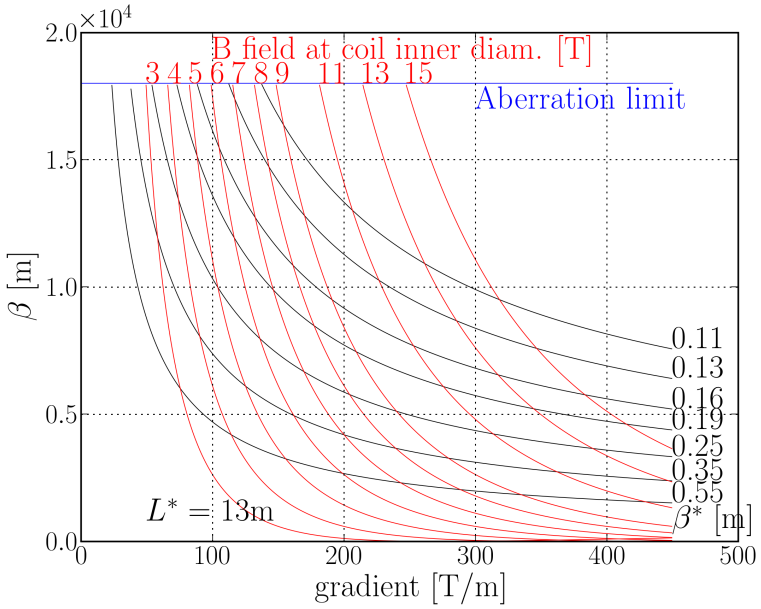

Figure 20: Triplet design. The figure shows the boundaries of the region in the maximum (β, gradient)-space, where it is possible to find a solution for a triplet or a quadruplet final focus system for the LHC. The regions are delimited by the pole field in the magnet (regions below the red lines) and the focusing ability (regions above the gray lines). L^* is 13 m. The plot can be used as a design guideline.

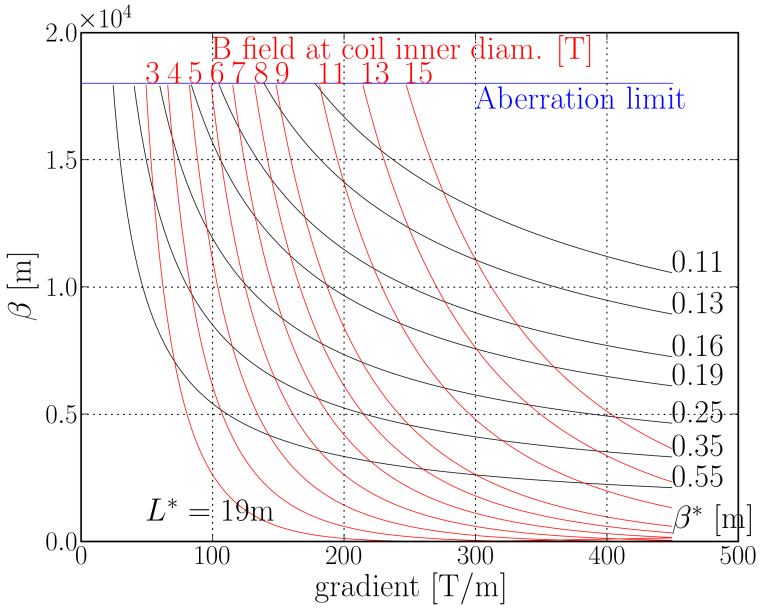

Figure 21: Triplet design. The figure shows the boundaries of the region in the maximum (β, gradient)-space, where it is possible to find a solution for a triplet or a quadruplet final focus system for the LHC. The regions are delimited by the pole field in the magnet (regions below the red lines) and the focusing ability (regions above the gray lines). L^* is 19 m. The plot can be used as a design guideline.

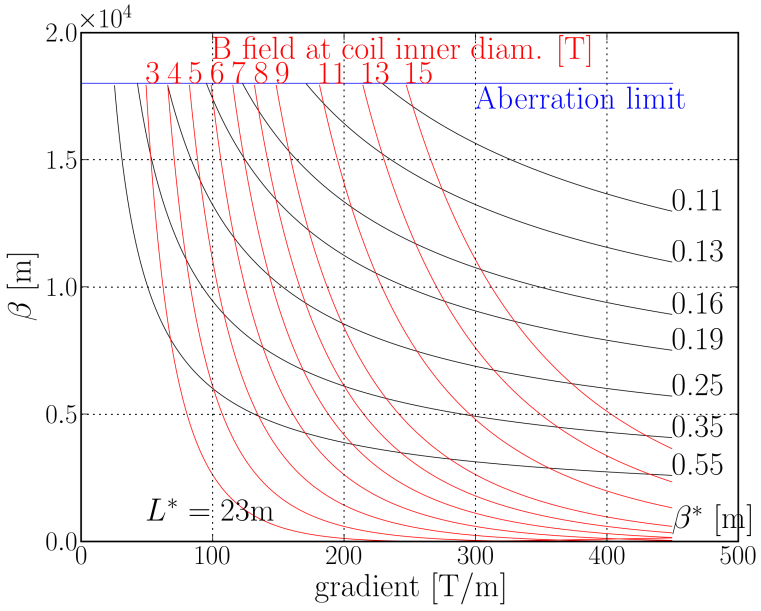

Figure 22: Triplet design. The figure shows the boundaries of the region in the maximum (β, gradient)-space, where it is possible to find a solution for a triplet or a quadruplet final focus system for the LHC. The regions are delimited by the pole field in the magnet (regions below the red lines) and the focusing ability (regions above the gray lines). L^* is 23 m. The plot can be used as a design guideline.

11 Parameter space

All previous estimates define the region in the parameter space for a realistic final focus (regions above the black lines and below the blue and red lines in Fig. 19). Fig. 19 shows in addition the matched optics presented in [20] and the nominal optics. One can see how their parameters fit the ones predicted by the method although the matched optics does not strictly use the same layout. The nominal layout, using NbTi quadrupoles whose peak field in the coil exceeds 6.5 T, is on the left of the 6.5 T line.

Figures 20, 21, 22 give a detailed description of the parameter space for several L^*.

12 Conclusions

A constant gradient point to parallel final focus is a simple model whose parameter can be found for any initial conditions through a set of functions of one parameter. These functions are the solutions of a system of equations that can be solved numerically and can be used as a design tool.

Some solutions are compared in terms of maximum beta function, total length and chromaticity.

The approximation and properties stated so far are always valid for a final focus system and allow to write simpler conditions compared to the exact theory.

A realistic implementation of the layouts can be derived including the necessary gaps between the quadrupoles. This will change the layout parameters and increases the maximum beta, total length and chromaticity. As long as the gap lengths are smaller than the magnet lengths, the effect is small if the integrated strengths are kept constant.

The method and the results can be used for exploring systematically the expected performance in terms of maximum beta, total length and chromaticity of a final focus system for which the pole field of the magnet is one of the limitation. In addition the method determines the layout parameter such as length, position and gradient of the magnets.

The analysis was concluded for the case of the LHC in the framework of the LHC IR upgrade studies. The conditions for an effective final focus system are combined with the constraints coming from the magnet technology and the LHC machine parameters. The results show the set of layout parameters compatible with the NbTi or Nb_3Sn technology and the expected performance. The predictions are compared with several realistic designs showing a good agreement with the analysis.

13 Acknowledgments

I am grateful to Oliver Bruening for encouraging me to study this topic and the initial discussion. Steve Peggs and Stephane Fartoukh for suggesting me to use the simplified differential equation for ν (Eq. (12)) and Stephane in particular for the use of the scaling in Eq. (36),(37). I would like to thank Massimo Giovannozzi, Werner Herr, Ulrich Dorda and Leonid Rivkin for the patient review of this paper.

References

[1] E. D. Courant and H. S. Snyder. Theory of the alternating-gradient synchrotron. *Annals of Physics*, 1(3):1–48, jan 1958.

[2] E. Regenstreif. Phase-space transformations by means of quadrupole multiplets. CERN 67-6, CERN, March 1967.

[3] E. Regenstreif. Possible and impossible phase-space transformations by means of alternating-gradient doublets and triplets. CERN 67-8, CERN, March 1967.

[4] Karl L. Brown and Roger V. Servranckx. First and second order charged particle optics. Technical Report SLAC-PUB-3381, SLAC, July 1984.

[5] Karl L. Brown and Roger V. Servranckx. Optics modules for circular accelerator design. *Nuclear Instruments and Methods in Physics Research Section A: Accelerators, Spectrometers, Detectors and Associated Equipment*, 258(3):480–502, August 1987.

[6] P. Raimondi and Andrei Seryi. Novel final focus design for future linear colliders. *Phys. Rev. Lett.*, 86(17):3779 – 3782, apr 2001.

[7] R. de Maria, O. Bruening, and P. Raimondi. LHC IR upgrade: A dipole first option with local chromaticity correction. Technical Report CERN-LHC-Project-Report-934, CERN, June 2006. Presented at: European Particle Accelerator Conference EPAC'06 , Edinburgh, Scotland, UK , 26 - 30 Jun 2006.

[8] J.D. Jackson, R.G. Barton, and R. Donaldson. Conceptual design of the superconducting super collider. Technical Report SSC-SR–2020, SSC Central Design Group, March 1986.

[9] O. Bruening, P. Collier, P. Lebrun, S. Myers, R. Ostojic, J. Poole, and P. Proudlock. LHC design report. Technical Report CERN-2004-003, CERN, 2004.

[10] Oliver Sim Bruening, Roberto Cappi, R. Garoby, O. Groebner, W. Herr, T. Linnecar, R. Ostojic, K. Potter, L. Rossi, F. Ruggiero, Karlheinz Schindl, Graham Roger Stevenson, L. Tavian, T. Taylor, Emmanuel Tsesmelis, E. Weisse, and Frank Zimmermann. LHC luminosity and energy upgrade : A feasibility study. Technical Report LHC-Project-Report-626, CERN, December 2002.

[11] F. Ruggiero, W. Scandale, and F. Zimmermann, editors. *First CARE-HHH-APD Workshop on Beam Dynamics in Future Hadron Colliders and Rapidly Cycling High-Intensity Synchrotrons*, number CERN-2005-006, 2004.

[12] F. Ruggiero, W. Scandale, and F. Zimmermann, editors. *Second CARE-HHH-APD Workshop on Scenarios for the LHC Luminosity Upgrade*, number CERN-2006-008. CERN, 2005.

[13] W. Scandale, T. Taylor, and F. Zimmermann, editors. *Third CARE-HHH-APD Workshop on Towards a Roadmap for the Upgrade of the LHC and GSI Accelerator Complex*, number CERN-2007-002. CERN, 2006.

[14] E. T. d'Amico and G. Guignard. Analysis of a symmetric triplet and its application to ring insertions. CLIC-Note 341, CERN, May 1997.

[15] E.T. d'Amico and G. Guignard. Analysis of generic insertions made of two symmetric triplets. CERN-SL 98-014, CERN, May 1998.

[16] S. Peggs. Minimising chromaticity in interaction regions with long weak quadrupoles. In *SSC Summer Study*, 1984.

[17] J. P. Koutchouk, L. Rossi, and E. Todesco. A solution for phase-one upgrade of the LHC low-beta quadrupoles based on nb-ti. lhc-project-report 1000, CERN, April 2007.

[18] R. Ostojic, N. Catalan Lasheras, G. Kirby, and S. Russenschuck. Low-beta quadrupole designs for the LHC luminosity upgrade. In *PAC05*, 2005.

[19] F. Ruggiero, O. Bruening, R. Ostojic, L. Rossi, W. Scandale, T. Taylor, and A. Devred. Performance limits and IR design of a possible LHC luminosity upgrade based on Nb-Ti SC magnet. In *EPAC04*, 2004.

[20] O. Bruening, R. de Maria, and R. Ostojic. Low gradient, large aperture ir upgrade options for the lhc compatible with nb-ti magnet technology. LHC-Report 1008, CERN, jun 2007.

[21] L. Rossi and E. Todesco. Electromagnetic design of superconducting quadrupoles. *Phys Rev ST Accel and Beams*, 9(10):20, October 2006.

[22] R. de Maria and O. Bruening. A low gradient quadrupole first layout compatible with nbti magnet technology and beta*= 0.25m. Technical Report CERN-LHC-Project-Report-933, CERN, June 2006. Presented at: European Particle Accelerator Conference EPAC'06 , Edinburgh, Scotland, UK , 26 - 30 Jun 2006.